Main Chain Polymers Containing Banana-Shaped Mesogens: Synthesis and Mesomorphic Properties

E-Joon Choi,*,† Jae-Chul Ahn,† Liang-Chy Chien,‡ Chong-Kwang Lee,*,§,○ Wang-Cheol Zin,⊥,⊗ Dae-Cheol Kim,⊥ and Sung-Tae Shin∥

Department of Polymer Science and Engineering, Kumoh National Institute of Technology, Kumi, Kyungbuk 730-701, Korea, Liquid Crystal Institute, Kent State University, Kent, Ohio 44242, Department of Chemistry, Gyeongsang National University, Chinju 660-701, Korea, Department of Materials Science and Engineering, Pohang University of Science and Technology, Pohang 790-784, Korea, and Department of Physics, Korea University, Chungnam 339-700, Korea

Received June 16, 2003; Revised Manuscript Received October 21, 2003

ABSTRACT: Twelve azomethine polymers containing a banana-shaped mesogen as a repeating unit have been synthesized by polycondensation, and their mesomorphic properties were studied. The solution viscosities were measured in a 0.16 g/dL solution in H_2SO_4 at 30 °C, and the values are in the range 0.37−0.79 dL/g. Polymers obtained were characterized by FT/IR and NMR spectrometry, differential scanning calorimetry (DSC), optical microscopy, and X-ray diffractometry (XRD). The effect of spacer length and lateral substituents on the central core as well as the sidearms of these polymers are described. Of the 12 polymers, eight polymers are found to be thermotropic liquid crystals. Among four polymers with a dioxydodecamethylenene spacer, three polymers exhibited banana phases and one polymer revealed a smectic phase; four polymers with a dioxyhexamethylene spacer showed only a nematic phase. The structures of the banana phases in the polymers are also described.

Introduction

Since Meyer et al.[1] discovered ferroelectricity in tilted smectic phases of chiral molecules, helicity, or chirality has been a most attractive subject in the research field of liquid crystals.[2−6] As predicted by theoretical studies, when any structural factors can reduce the overall symmetry of the mesophase, the helicity or chirality of mesophase could appear even in liquid crystal systems without chemical chirality. In 1996, Niori et al.[7] observed the first obvious example of ferroelectricity in a smectic phase formed by achiral banana-shaped molecules. Subsequently, Link et al.[4] found spontaneous formation of macroscopic chiral domains in a fluid smectic phase derived from achiral molecules with bent cores. In 1997, at a conference in Berlin,[8] the banana phases were tentatively named with the code letters B_1 to B_7 according to the order of discovery, which should not be mixed up with the notation of B for a smectic mesophase of rodlike molecules. The B_1 phase has a two-dimensional rectangular structure.[9,10] The B_2 phase is a fluid smectic phase associated with antiferroelectric characteristics.[4,11] The B_3 phase has been shown to be crystalline, and thus it should be excluded from a nomenclature for banana phases.[12] It is still in dispute whether the B_4 phase is a real crystalline phase or some type of high order liquid crystalline phase.[13] The B_5 phase is a titled smectic phase which has been observed in only a few compounds,[14] and the B_6 phase is an intercalated smectic C phase.[10,12] The B_7 phase shows helical ribbons in the optical texture and ferroelectric characteristics.[15,16] Significantly, we have discovered a helical superstructure in the B_7 phase.[17] Over the past few years, a considerable number of studies have been made on the relationship between the structure and properties for the compounds composed of bent cores such as banana-shaped molecules.[18−30] On the other hand, little attention has been given to polymeric materials containing banana-shaped mesogenic moiety. So far, there are no reports of the synthesis and characterization of liquid crystalline polymers having banana-shaped mesogenic units in the main chain.[31]

In this paper, we report the synthesis of 12 different azomethine polymers consisting of banana-shaped mesogen and characterization of their mesophase, as well as the effect of space length and lateral halogen substituents. As a strategy to manipulate the banana phase accessed by main chain polymers, we have chosen a five-ring system such as 1,3-phenylene bis[4-(3-chloro-4-*n*-octyloxyphenyliminomethyl)benzoate][17] or 1,3-phenylene bis[4-(3-fluoro-4-*n*-octyloxyphenylimino-methyl)benzoate][11] as a model compound, since these compounds form banana phases and exhibit ferroelectricity (or antiferroelectricity). The synthetic details include (1) varying the carbon number (m = 6 or 12) of the alkylene flexible spacer, (2) introducing two chorine substituents (X = Cl) on the central phenylene unit, and (3) introducing a fluorine or chlorine substituent (Y = F or Cl) into the outer phenylene unit. For comparison, unsubstituted parent polymers (X and Y = H) also were synthesized.

Experimental Section

Synthesis. Synthetic route to azomethine polymers containing banana-shaped mesogen is shown in Scheme 1. Since the synthetic procedures used to prepare the polymers were essentially the same, one representative polymer is given in the following. All spectral data of the other polymers are also included.

Synthesis of 1,3-Phenylene Bis(4-formylbezoate).[32] Yield: 62%. IR (KBr pellet, cm^{-1}): 3100 (aromatic =CH, st),

* Corresponding author. E-mail: ejchoi@kumoh.ac.kr.
† Kumoh National Institute of Technology.
‡ Kent State University.
§ Gyeongsang National University.
⊥ Pohang University of Science and Technology.
∥ Korea University.
⊗ E-mail: wczin@postech.ac.kr.
○ E-mail: cklee@nongae.gsnu.ac.kr.

10.1021/ma0348122 CCC: $27.50
Published on Web 12/13/2003

Scheme 1. Synthetic Route to Azomethine Polymers

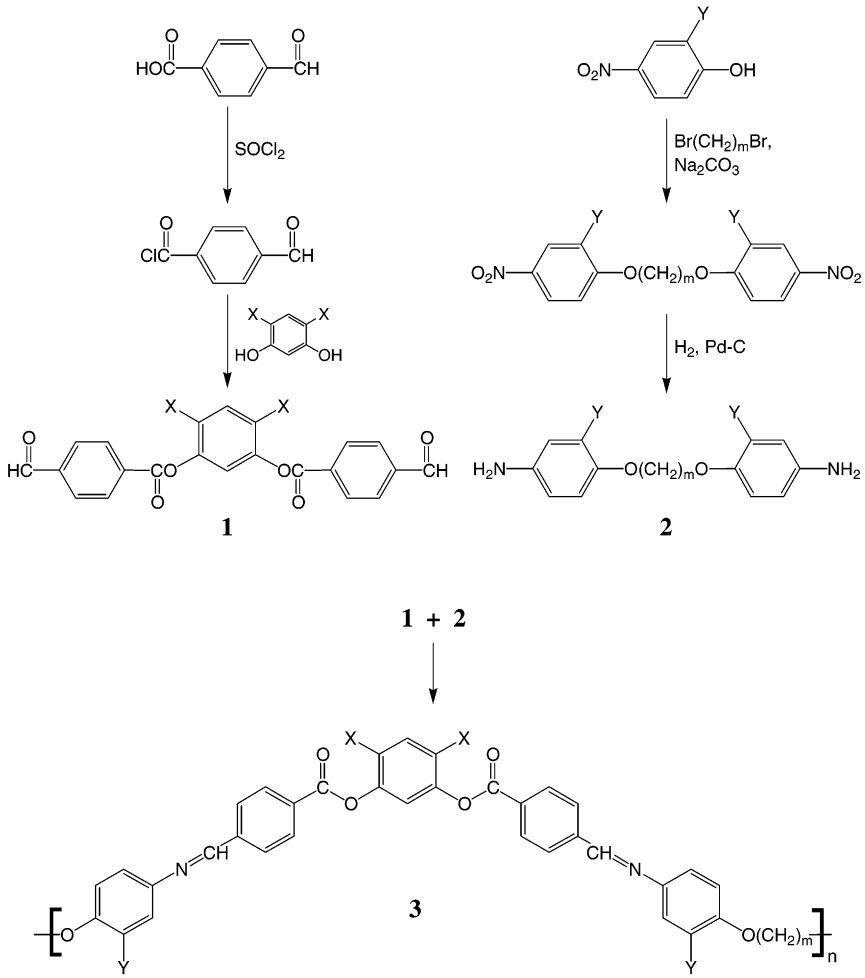

	3a	3b	3c	3d	3e	3f	3g	3h	3i	3j	3k	3l
m	6	6	6	6	6	6	12	12	12	12	12	12
X	H	H	H	Cl	Cl	Cl	H	H	H	Cl	Cl	Cl
Y	H	F	Cl	H	F	Cl	H	F	Cl	H	F	Cl

2850, 2750 (aldehyde CH, st) 1740 (ester C═O, st), 1704 (aldehyde C═O, st), 1610, 1600 (aromatic C═C, st), 1270, 1200, 1140, 1020 (CO, st). ^{1}H NMR ($CDCl_3$, δ in ppm): 10.26 (2H, s, C*H*O), 8.49−8.35 (4H, d, Ar*H*), 8.16−8.02 (4H, d, Ar*H*), 7.56−7.49 (1H, t, Ar*H*), 7.27−7.19 (3H, m, Ar*H*).

Synthesis of 4,6-Dichloro-1,3-phenylene Bis(4-formylbenzoate).[33] Yield: 67%. IR (KBr pellet, cm^{-1}): 3100 (aromatic ═CH, st), 2840, 2730 (aldehyde CH, st), 1742 (ester C═O), 1702 (aldehyde C═O, st), 1579, 1478 (aromatic C═C, st), 1254, 1201, 1159, 1018 (CO, st). ^{1}H NMR ($CDCl_3$, δ in ppm): 10.16 (2H, s, C*H*O), 8.41−8.37 (4H, d, Ar*H*), 8.08−8.03 (4H, d, Ar*H*), 7.69 (1H, s, Ar*H*), 7.43 (1H, s, Ar*H*).

Synthesis of 1,6-bis(4-aminophenoxy)hexane. 1,6-Bis-(4-nitrophenoxy)hexane[34] (2.0 g, 5.6 mmol), 0.5 g of 5% palladium on carbon, and 200 mL of ethanol were placed in a 1 L pressurized reaction vessel. Under 100 psi of hydrogen pressure, the mixture was stirred at 80 °C for 3 h. After the reaction vessel was relieved from the hydrogen pressure, the catalyst was filtered off. Then the filtrate was concentrated using a rotatory evaporator. The white solid obtained was recrystallized from ethanol to give the pure product. Yield: 82%. IR (KBr pellet, cm^{-1}): 3393, 3310 (NH_2, st), 3015 (aromatic ═CH, st), 2933 (aliphatic CH, st), 1642 (NH, bend), 1517, 1472 (aromatic C═C, st), 1237, 1179, 1118, 1009 (CO, st). ^{1}H NMR (DMSO-d_6, δ in ppm); 6.63−6.59 (4H, d, Ar*H*), 6.49−6.45 (4H, d, Ar*H*), 4.55(4H, s, NH_2), 3.82−3.76 (4H, t, OCH_2), 1.64 (4H, br s, OCH$_2$CH_2), 1.41 (4H, br s, OCH$_2$-CH$_2$CH_2).

Synthesis of Polymer 3a. 1,3-Phenylene bis(4-formylbenzoate) (0.63 g, 2.10 mmol) and 1,6-bis(4-aminophenoxy)hexane (0.78 g, 2.10 mmol) were dissolved in 40 mL of dry dichloromethane and evaporated to dryness. The residue was dissolved in a mixture (50 mL) of 1-methyl-2-pyrrolidinone and hexamethylphosphoramide (4:1 v/v). The solution was heated to 120 °C with stirring for 12 h. After cooling, the reaction mixture was poured into methanol, and the formed precipitate was washed with water and methanol thoroughly and dried under vacuum at 60 °C. Yield: 95%. IR (KBr pellet, cm^{-1}): 3065 (aromatic ═CH, st), 2934, 2865 (aliphatic CH, st), 1735 (C═O, st), 1680 (C═N, st), 1622, 1501 (aromatic C═C, st), 1245, 1134, 1065 (CO, st). ^{1}H NMR spectrum (CF_3CO_2D, δ in ppm): 9.28 (2H, s, N═C*H*), 8.60−8.55 (4H, d, Ar*H*), 8.39−8.35 (4H, d, Ar*H*), 7.80−7.76 (4H, d, Ar*H*), 7.64 (1H, br s, Ar*H*), 7.30−7.18 (7H, m, Ar*H*), 4.21 (4H, br s, OCH_2), 1.96 (4H, br s, OCH$_2$CH_2), 1.65 (4H, br s, OCH$_2$CH$_2$CH_2).

Synthesis of Polymer 3b. Yield: 91%. IR (KBr pellet, cm^{-1}): 3058 (aromatic ═CH, st), 2924, 2852 (aliphatic CH, st), 1738 (C═O, st), 1680 (C═N, st), 1618, 1500 (aromatic C═C, st), 1241, 1102, 1080, 1011 (CO, st). ^{1}H NMR spectrum (CF_3-CO_2D, δ in ppm): 9.33 (2H, s, N═C*H*), 8.61 (4H, br s, Ar*H*),

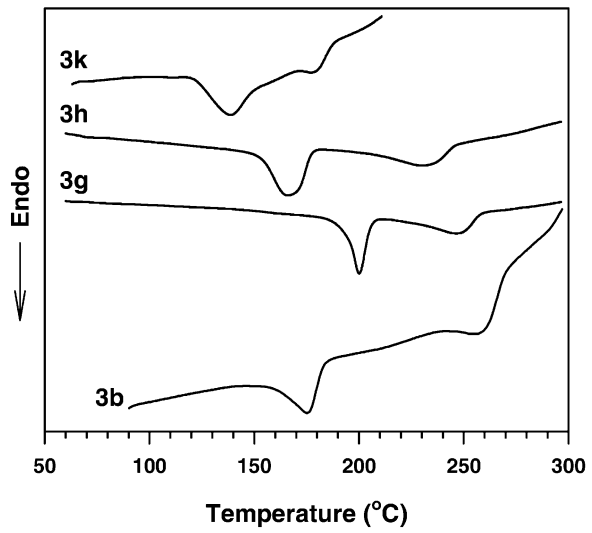

Figure 1. DSC thermograms for polymers **3b**, **3g**, **3h**, and **3k** showing typical T_m and T_i transitions (heating rate: 20 °C/min).

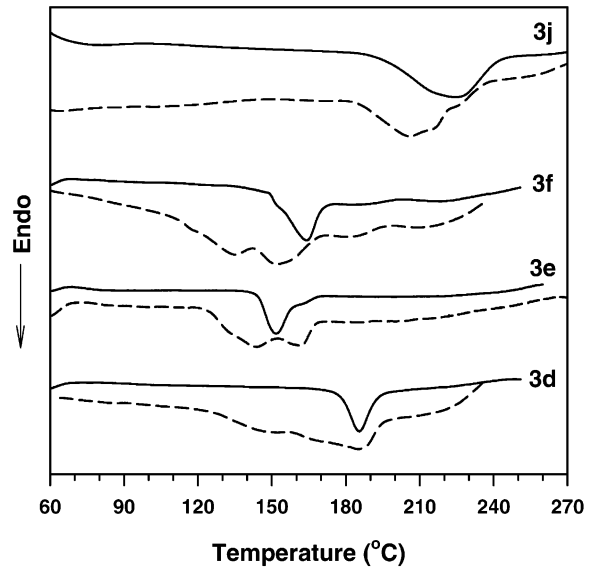

Figure 2. DSC thermograms for polymers **3d**, **3e**, **3f**, and **3j** obtained on first heating (dashed line) and after preheating for 1 h (solid line).

8.42−8.29 (4H, d, Ar*H*), 7.82 (2H, br s, Ar*H*), 7.69 (1H, br s, Ar*H*), 7.35−7.24 (7H, m, Ar*H*), 4.27 (4H, br s, OCH_2), 2.00 (4H, br s, OCH$_2$CH_2), 1.70 (4H, br s, OCH$_2$CH$_2$CH_2).

Synthesis of Polymer 3c. Yield: 88%. IR (KBr pellet, cm^{-1}): 3059 (aromatic =CH, st), 2928, 2852 (aliphatic CH, st), 1738 (C=O, st), 1688 (C=N, st), 1621, 1508 (aromatic C=C, st), 1241, 1122, 1081, 1004 (CO, st). ^{1}H NMR spectrum (CF$_3$CO$_2$D, δ in ppm): 9.33 (2H, s, N=C*H*), 8.62−8.58 (4H, d, Ar*H*), 8.43−8.38 (4H, d, Ar*H*), 7.77−7.63 (5H, m, Ar*H*), 7.31 (5H, br s, Ar*H*), 4.30 (4H, s, OCH_2), 1.99 (4H, br s, OCH$_2$CH_2), 1.77 (4H, br s, OCH$_2$CH$_2$CH_2).

Synthesis of Polymer 3d. Yield: 93%. IR (KBr pellet, cm^{-1}): 3048 (aromatic =CH, st), 2926, 2852 (aliphatic CH, st), 1741 (C=O, st), 1689 (C=N, st), 1619, 1501 (aromatic C=C, st), 1239, 1150, 1058, 1111 (CO, st). ^{1}H NMR spectrum (CF$_3$CO$_2$D, δ in ppm): 9.53 (2H, br s, N=C*H*), 8.42−8.38 (4H, d, Ar*H*), 8.34−8.28 (4H, d, Ar*H*), 7.88−7.84 (4H, d, Ar*H*), 7.60 (1H, s, Ar*H*), 7.33−7.28 (5H, d, Ar*H*), 4.17 (4H, br s, OCH_2), 2.04 (4H, br s, OCH$_2$CH_2), 1.74 (4H, br s, OCH$_2$CH$_2$CH_2).

Synthesis of Polymer 3e. Yield: 92%. IR (KBr pellet, cm^{-1}): 3050 (aromatic =CH, st), 2924, 2851 (aliphatic CH, st), 1739 (C=O, st), 1687 (C=N, st), 1618, 1502 (aromatic C=C, st), 1242, 1164, 1062, 1018 (CO, st). ^{1}H NMR spectrum (CF$_3$CO$_2$D, δ in ppm): 9.53−9.49 (2H, d, N=C*H*), 8.86−8.82 (4H, d, Ar*H*), 8.65−8.61 (4H, m, Ar*H*), 8.15−8.11 (2H, br s, Ar*H*), 7.90 (1H, s, Ar*H*), 7.49−7.36 (5H, m, Ar*H*), 4.50 (4H, br s, OCH_2), 2.22 (4H, br s, OCH$_2$CH_2), 1.91 (4H, br s, OCH$_2$CH$_2$CH_2).

Synthesis of Polymer 3f. Yield: 84%. IR (KBr pellet, cm^{-1}): 3058 (aromatic =CH, st), 2924, 2851 (aliphatic CH, st), 1740 (C=O, st), 1679 (C=N, st), 1620, 1512 (aromatic C=C, st), 1241, 1148, 1059, 1004 (CO, st). ^{1}H NMR spectrum (CF$_3$CO$_2$D, δ in ppm): 9.56−9.53 (2H, d, N=C*H*), 8.89−8.85 (4H, d, Ar*H*), 8.69−8.65 (4H, d, Ar*H*), 8.14−7.75 (5H, m, Ar*H*), 7.59−7.36 (3H, m, Ar*H*), 4.56 (4H, br s, OCH_2), 2.26 (4H, br s, OCH$_2$CH_2), 1.96 (4H, br s, OCH$_2$CH$_2$CH_2).

Synthesis of Polymer 3g. Yield: 87%. IR (KBr pellet, cm^{-1}): 3071 (aromatic =CH, st), 2920, 2844 (aliphatic CH, st), 1738 (C=O, st), 1684 (C=N, st), 1620, 1504 (aromatic C=C, st), 1244, 1128, 1062, 1018 (CO, st). ^{1}H NMR spectrum (CF$_3$CO$_2$D, δ in ppm): 9.55 (2H, s, N=C*H*), 8.88−8.84 (4H, d, Ar*H*), 8.67−8.63 (4H, d, Ar*H*), 8.08−8.04 (4H, d, Ar*H*), 7.93 (1H, br s, Ar*H*), 7.62−7.48 (7H, m, Ar*H*), 4.52−4.46 (4H, t, OCH_2), 2.18 (4H, br s, OCH$_2$CH_2), 1.67 (16H, br s, OCH$_2$CH$_2$(CH_2)$_4$).

Synthesis of Polymer 3h. Yield: 91%. IR (KBr pellet, cm^{-1}): 3072 (aromatic =CH, st), 2922, 2844 (aliphatic CH, st), 1738 (C=O, st), 1694 (C=N, st), 1599, 1504 (aromatic C=C,

Table 1. Yields, Solution Viscosities, and Melting Temperatures of Polymers[a]

polymer (*m*/X/Y)	yield (wt %)	η_{inh} [b] (dL/g)	T_m (°C)	ΔH_m [c] (J/g)
3a (6/H/H)	95	0.48	215	3.4
				12.6
3b (6/H/F)	91	0.48	176	12.9
3c (6/H/Cl)	88	0.79	215	8.9
3d (6/Cl/H)	93	0.51	186	8.6
				13.7
3e (6/Cl/F)	92	0.48	163	12.7
				10.9
3f (6/Cl/Cl)	84	0.46	184	12.8
				10.8
3g (12/H/H)	87	0.49	200	25.9
3h (12/H/F)	91	0.48	166	26.0
3i (12/H/Cl)	89	0.52	172	16.6
				18.7
3j (12/Cl/H)	92	0.45	224	36.6
				36.5
3k (12/Cl/F)	88	0.37	138	12.2
3l (12/Cl/Cl)	93	0.43	120	9.1

[a] The values in italics are data for heat-treated samples at the given temperature for 1 h: **3a** (175 °C); **3d** (160 °C); **3e** (130 °C); **3f** (145 °C); **3i** (120 °C); **3j** (175 °C). [b] Measured on 0.16 g/dL solution in sulfuric acid at 30 °C. [c] Total enthalpy changes for multiple melting endotherms.

Table 2. Transition Temperatures (°C) and Enthalpy Changes for Isotropization (J/g) (in Parentheses)[a]

polymer	phase behavior
3a	Cr 215 I
3b	Cr 176 N 259 (7.9) I
3c	Cr 215 I
3d	Cr 186 N (b) I
3e	Cr 163 N (b) I
3f	Cr 184 N (b) I
3g	Cr 200 B_2 248 (15.9) I
3h	Cr 166 SmA 231 (14.0) I
3i	Cr 172 I
3j	Cr 224 B_1 (b) I
3k	Cr 138 B_1 179 (9.0) I
3l	Cr 120 I

[a] Cr = crystalline phase; N = nematic phase; SmA = smectic A phase; B_1 = rectangular tilted banana phase; B_2 = lamellar tilted banana phase; I = isotropic phase. [b] Thermal decomposition occurred before the mesophase-to-isotropic transition.

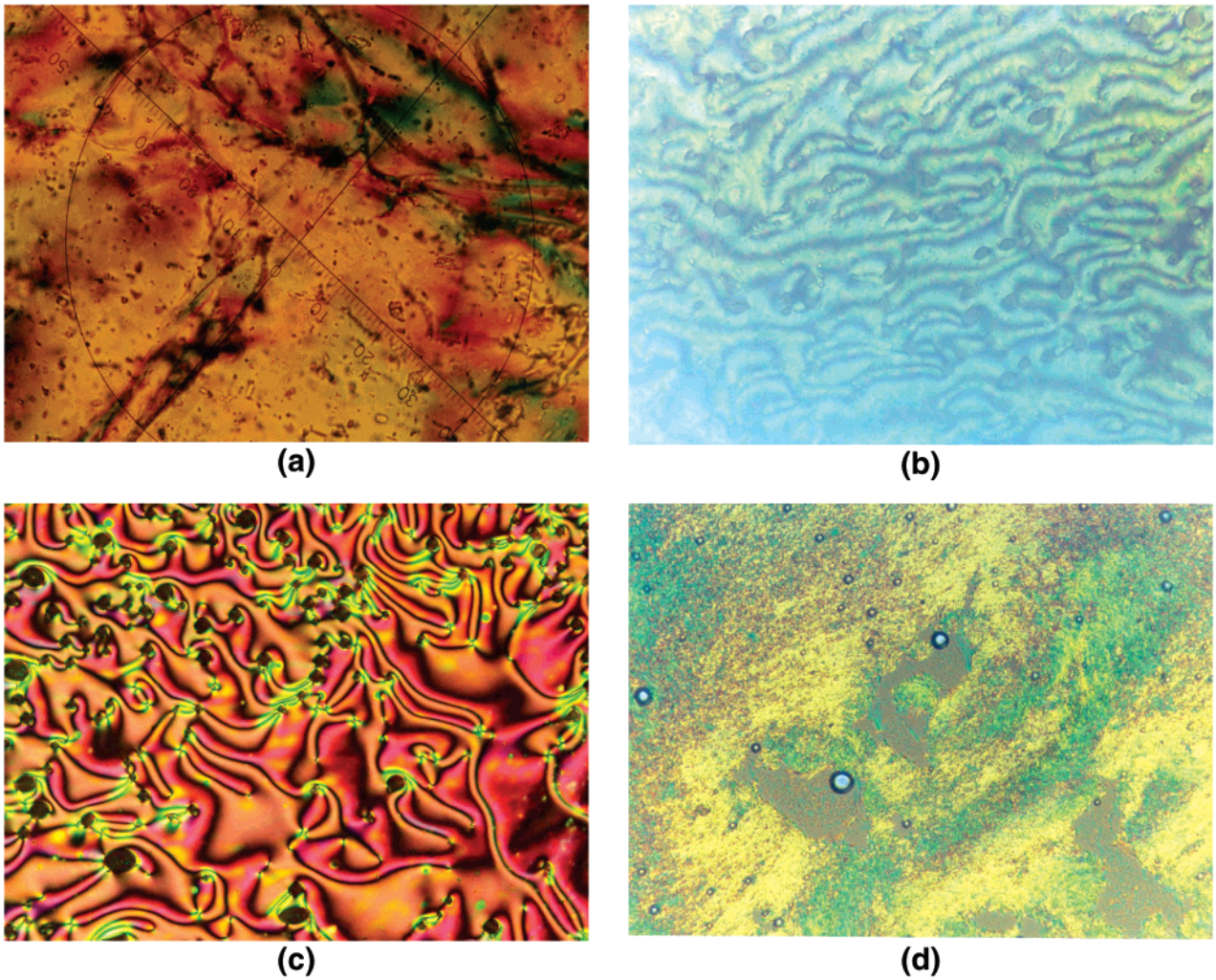

Figure 3. Optical microscopic textures for the nematic phases of polymers, magnification ×200: (a) **3b** (238 °C), (b) **3d** (219 °C), (c) **3e** (220 °C), and (d) **3f** (194 °C).

st), 1242, 1123, 1060, 1008 (CO, st). ^{1}H NMR spectrum (CF_3CO_2D, δ in ppm): 9.52 (2H, s, N=C*H*), 8.81−8.48 (8H, m, Ar*H*), 7.89 (2H, br s, Ar*H*), 7.82 (1H, br s, Ar*H*), 7.54−7.31 (7H, m, Ar*H*), 4.56 (4H, m, OCH_2), 2.16 (4H, br s, OCH$_2$CH_2), 1.63 (16H, br s, OCH$_2$CH$_2$(CH_2)$_4$).

Synthesis of Polymer 3i. Yield: 89%. IR (KBr pellet, cm^{-1}): 3078 (aromatic =CH, st), 2921, 2848 (aliphatic CH, st), 1738 (C=O, st), 1682 (C=N, st), 1620, 1508 (aromatic C=C, st), 1242, 1122, 1061, 1008 (CO, st). ^{1}H NMR spectrum (CF_3CO_2D, δ in ppm): 9.55 (2H, s, N=C*H*), 8.86−8.81 (4H, d, Ar*H*), 8.66−8.62 (4H, d, Ar*H*), 8.01−7.92 (5H, m, Ar*H*), 7.49 (5H, br s, Ar*H*), 4.55−4.48 (4H, t, OCH_2), 2.18 (4H, br s, OCH$_2$CH_2), 1.64 (16H, br s, OCH$_2$CH$_2$(CH_2)$_4$).

Synthesis of Polymer 3j. Yield: 92%. IR (KBr pellet, cm^{-1}): 3070 (aromatic =CH, st), 2921, 2944 (aliphatic CH, st), 1741 (C=O, st), 1698 (C=N, st), 1618, 1502 (aromatic C=C, st), 1242, 1160, 1059, 1018 (CO, st). ^{1}H NMR spectrum (CF_3CO_2D, δ in ppm): 9.54−9.49 (2H, d, N=C*H*), 8.88−8.55 (8H, m, Ar*H*), 8.04−7.93 (4H, d, Ar*H*), 7.81 (1H, s, Ar*H*), 7.50−7.46 (5H, d, Ar*H*), 4.33 (4H, br s, OCH_2), 2.02 (4H, br s, OCH$_2$CH_2), 1.65 (16H, br s, OCH$_2$CH$_2$(CH_2)$_4$).

Synthesis of Polymer 3k. Yield: 88%. IR (KBr pellet, cm^{-1}): 3068 (aromatic =CH, st), 2921, 2822 (aliphatic CH, st), 1742 (C=O, st), 1678 (C=N, st), 1620, 1502 (aromatic C=C, st), 1242, 1168, 1062, 1018 (CO, st). ^{1}H NMR spectrum (CF_3CO_2D, δ in ppm): 9.54−9.50 (2H, d, N=C*H*), 8.87−8.66 (8H, m, Ar*H*), 8.07 (2H, br s, Ar*H*), 7.81 (1H, s, Ar*H*), 7.46−7.36 (5H, m, Ar*H*), 4.48 (4H, br s, OCH_2), 2.18 (4H, br s, OCH$_2$CH_2), 1.65 (16H, br s, OCH$_2$CH$_2$(CH_2)$_4$).

Synthesis of Polymer 3l. Yield: 93%. IR (KBr pellet, cm^{-1}): 3074 (aromatic =CH, st), 2921, 2844 (aliphatic CH, st), 1742 (C=O, st), 1682 (C=N, st), 1621, 1512 (aromatic C=C, st), 1248, 1159, 1060, 1018 (CO, st). ^{1}H NMR spectrum (CF_3CO_2D, δ in ppm): 9.56−9.52 (2H, d, N=C*H*), 8.86−8.82 (4H, d, Ar*H*), 8.66−8.63 (4H, d, Ar*H*), 8.01−7.87 (5H, m, Ar*H*), 7.57−7.33 (3H, m, Ar*H*), 4.52 (4H, br s, OCH_2), 2.17 (4H, br s, OCH$_2$CH_2), 1.63 (16H, br s, OCH$_2$CH$_2$(CH_2)$_4$).

Characterization. IR and NMR spectra were obtained by Jasco 300E FT/IR and Bruker DPX 200 MHz NMR spectrometers, respectively. The phase transition temperatures were determined by differential scanning calorimeter (du Pont TA 910 DSC) and polarizing optical microscope (Zeiss, Jenapol). DSC measurements were performed in a N_2 atmosphere. The DSC heating and cooling rates were 20 °C/min. Optical textures were observed by the polarizing microscope equipped with a camera and a thermocontroller (Mettler FP82HT). X-ray analysis was performed in transmission mode with synchrotron radiation at the Pohang Accelerator Laboratory, Pohang, Korea. To investigate structural changes on heating, the sample was held in an aluminum sample holder which was sealed with a window of 7 μm thick Kapton films on both sides. The sample was heated with cartridge heaters and its temperature monitored by a thermocouple placed close to the sample. Subtracting the scattering from the Kapton gave a background scattering correction.

Results and Discussion

Synthesis and Mesogenic Properties. The synthetic route for the poly(azomethine)s is quite straightforward, and each reaction step is a relatively well-known type. For the polycondensation of diamine and

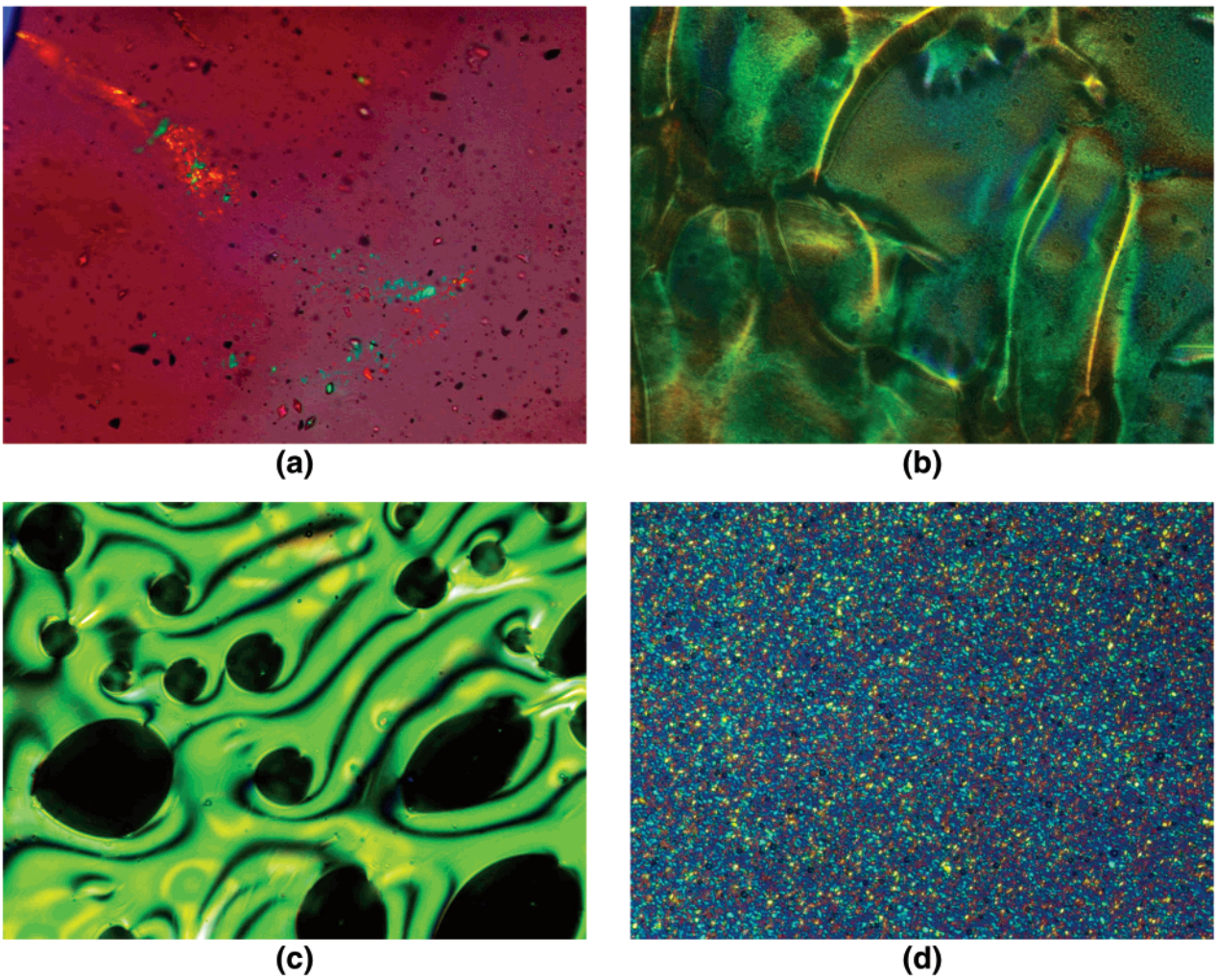

Figure 4. Optical microscopic textures for the smectic phases of polymers, magnification ×200: (a) **3g** (230 °C), (b) **3h** (200 °C), (c) **3j** (230 °C), and (d) **3k** (170 °C).

dialdehyde, two monomers were dissolved in dichloromethane, which was quickly evaporated to remain the powder mixture of the monomers without moisture. Then, the mixture of NMP/HMPA (4:1 v/v) was used for the polymerization solvent. Once a product was obtained as precipitate, all of the polymers were only soluble in strong acids, such as H_2SO_4, CF_3CO_2H, etc. The azomethine polymers obtained were characterized by IR and NMR spectroscopy. The spectral data were in accordance with the expected formula. The solution viscosities of the polymers were measured by using a 0.16 g/dL solution in sulfuric acid at 30 °C.[35,36] Although the solution was accompanied by an appreciable degree of decomposition, the inherent viscosity numbers were reasonably high in the range of 0.37−0.79 dL/g. Figures 1 and 2 display the DSC thermograms of the polymers. In Figure 1, four polymers (**3b**, **3g**, **3h**, and **3k**) exhibit the typical two endothermic peaks on their heating DSC thermograms, corresponding to the melting and isotropization transition, respectively. In Figure 2, four other polymers (**3d**, **3e**, **3f**, and **3j**) reveal multiple endothermic peaks on their heating DSC thermograms. To clear any ambiguity about the multiple endotherms either from mesomorphic polymorphism or from multiple melting phenomena, these polymers were preheated for 1 h at the onset point of the polymorph presumed to be a melting, respectively. As you can see from Figure 2, when the samples were thermally treated even for 1 h, among all polymorphs only one polymorph became distinctively intense. In Table 1, although the number of endothermic peaks decreased, the values of ΔH_m increased with preheated at onset point of the highest temperature polymorph. Otherwise, the values of ΔH_m slightly decreased. When the polymorph of the high temperature is for melting instead of isotropization, as preheated at the onset point of this polymorph, the ΔH_m increases because the polymer can have the optimal chain mobility to be crystallized, whereas as preheated at lower temperature than the onset point, the ΔH_m decreases because the intensity of the polymorph reduced. According to our XRD investigation, it is concluded that the multiple endothermic peaks are not related to polymesomorphic transitions. In Table 2, the enthalpy changes for isotropization (ΔH_i) of the former four polymers that could be determined is shown while for the latter four polymers a thermal decomposition occurs before the isotropization. As might be expected, the values of ΔH_i for smectic and banana phases are greater than those for a nematic phase. Another four polymers (**3a**, **3c**, **3i**, and **3l**) showed only one thermal transition (melting) due to their nonliquid crystallinity. Generally, the melting temperatures (T_m) decreased as the length of flexible spacer and the content of halogen substituent increased. The highest T_m is 224 °C for polymer **3j**, while the lowest T_m is 120 °C for polymer **3l**. Interestingly, the T_m of polymers with Y = F were

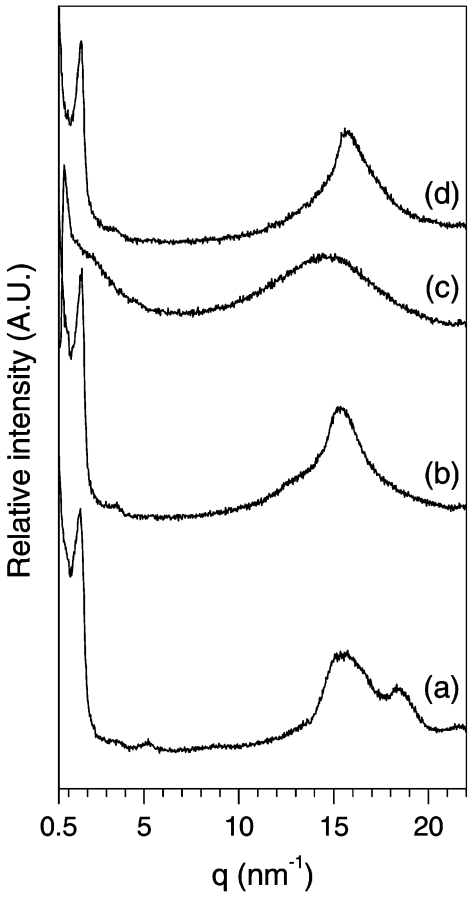

Figure 5. X-ray diffraction patterns for polymer **3g** measured at (a) room temperature, (b) 220 °C, and (c) 280 °C and following the heating, upon cooling the isotropic liquid, measured at (d) 80 °C.

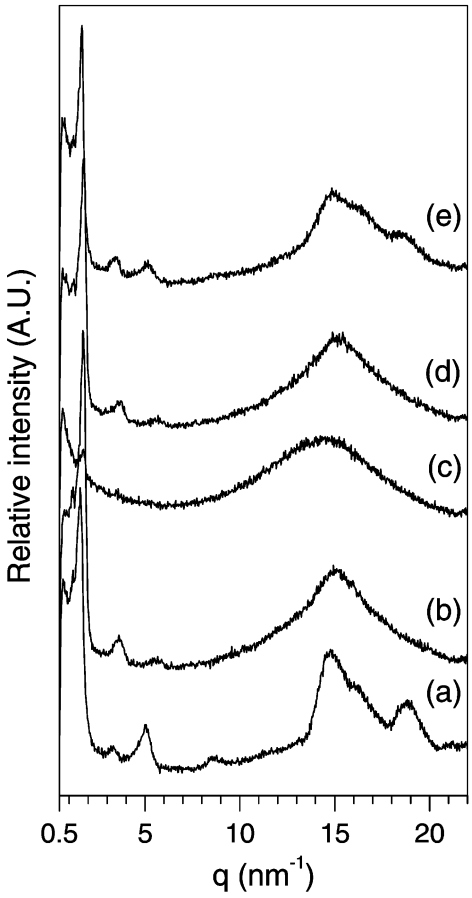

Figure 6. X-ray diffraction patterns for polymer **3h** measured at (a) room temperature, (b) 185 °C, and (c) 240 °C and ollowing the heating, upon cooling the isotropic liquid, measured at (d) 155 °C and (e) 80 °C.

comparable with those of polymers with Y = Cl. This might be attributed to the lower cohesive energy of the F atom than the Cl atom, though the F atom has a higher electronegativity and a smaller van der Waals radius than the Cl atom.

Microscopic Textures. When the spacer (*m*) is fixed at 6, four polymers (**3b**, **3d**, **3e**, and **3f**) are found to form a nematic phase. As shown in Figure 3, upon slow cooling the isotropic liquid at a rate of 1 °C/min, the polymers **3b** and **3f** exhibited a marble texture, while the polymers **3d** and **3e** revealed a schlieren texture which has both two and four brushes. The polymer **3a** unsubstituted and polymer **3c** with Y = Cl did not show birefringence in the melt state. Among the polymers with $m = 12$, four polymers (**3g**, **3h**, **3j**, and **3k**) did show birefringence in the melt state. To observe the optical texture in their viscous melt state, polymers **3g**, **3j**, and **3k** were slowly cooled at a rate of 0.5 °C/min, but extraordinarily in the case of polymer **3h** (Y = F), its optical texture could be observed only when the isotropic liquid is rapidly cooled. In Figure 4, optical micrographs of the polymers with $m = 12$ are presented. As can be seen, polymer **3j** (X = Cl) exhibits a schlieren texture with homeotropic domains which become birefringent when shear force is applied. The mesophases of the above four polymers with $m = 12$ could not be identified as banana phases only by their optical textures. The remaining two polymers with $m = 12$ and Y = Cl (**3i** and **3l**) did not reveal birefringence in the melt state.

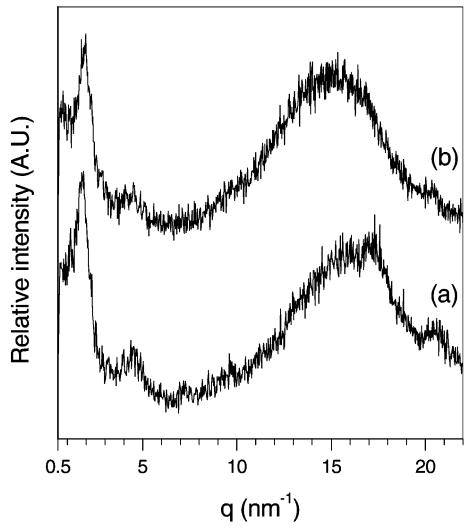

Figure 7. X-ray diffraction patterns for polymer **3k**: measured at (a) room temperature and (b) 160 °C.

X-ray Diffraction Studies. The nature of the liquid crystal phases has been confirmed by XRD studies. The melt state of the four polymers (**3b**, **3d**, **3e**, and **3f**) only showed liquidlike XRD patterns in wide- as well as small-angle regions. These mesophases with either schlieren or marble texture shown in Figure 3 have been identified as nematic phases. In Figures 5−7, for the other four polymers (**3g**, **3h**, **3j**, and **3k**), the representative XRD patterns obtained at given temperatures are

Table 3. X-ray Results for Polymers and the Structure of the Mesophase

polymer	Miller plane	*d* spacing (nm)
3g	(001)	$d = 3.67$
	(002)	
3h	(001)	$d = 4.65$
	(002)	
	(003)	
3j	(001)	$d_1 = 3.79$
	(100)	$d_2 = 1.82$
3k	(001)	$d_1 = 4.00$
	(100)	$d_2 = 1.85$

presented. In Figures 5−7, at room temperature, all of the polymers display crystalline XRD patterns, indicating a lamellar structure. When these polymers were heated to 220, 185, and 160 °C, respectively (above the transition temperatures of 200, 166, and 138 °C by DSC, in that order), in the small angle region, polymer **3g** has two peaks at $q = 1.71$ and 3.36 nm^{-1} (Figure 5b), polymer **3h** has three peaks at $q = 1.35$, 2.79, and 4.18 nm^{-1} (Figure 6b), and polymer **3k** has two peaks at $q = 1.59$ and 3.48 nm^{-1} (Figure 7b), while their entire wide angle regions exhibit only diffuse scattering. This is indicative of the smectic layer structure. When the polymers **3g** and **3h** were heated to 280 and 240 °C, respectively (above the transition temperatures of 248 and 231 °C by DSC, in that order), all reflections in the small angle region disappeared. By cooling isotropic melts, these two polymers retained the smectic layer structure as shown in Figures 5d and 6d. Note that only polymer **3h** could crystallize when cooled further (see Figure 6e). In the case of polymers **3j** and **3k**, cooling experiments could not be achieved due to thermal decomposition at the temperature of the isotropic state.

In Table 3, Miller planes and *d* spacings for mesophases of the four polymers (**3g**, **3h**, **3j**, and **3k**) are summarized. In the small angle region, polymer **3g** shows two reflections in the ratio 1:2, which are indexed as (001) and (002). The layer spacing (*d*) was measured to be 3.67 nm, indicating tilt of the molecules. As the length of repeating unit was measured as 4.6 nm by assuming the polymethylene chain to be fully extended in the all-trans-conformation, the tilt of the molecules was estimated to be about 40°. Similarly, Watanabe et al.[9] reported that B_2 phase of the compound with *m*/X/Y = 7/H/H only gave two reflections indexed as (001) and (002) with a missing (003) plane. Although the XRD patterns of the mesophase formed by polymer **3g** can be compared with those of model compounds already reported, the existence of the B_2 phase could not be directly proven, because the melt viscosity of the polymer is too high to investigate its switching properties. Furthermore, Pelzl et al.[37] reported that the compound with *m*/Y = 8/H and one Cl atom in the central core (X = mono-Cl) had three equally spaced reflections (three orders) indexed as (001), (002), and (003), whereas we[11] reported that the compound with *m*/X/Y = 8/H/F showed three reflections in the small angle region with an integral spacing ratio. In Table 3, polymer **3h** shows three reflections in the ratio 1:2:3, which are indexed as (001), (002), and (003). Nevertheless, we could not have presumed that polymer **3h** gives a B_2 phase without the tilt of the molecules. This mesophase has been identified merely as a smectic A phase with $d = 4.65$ nm. In the Table 3, in the small angle region, polymers **3j** and **3k** show two reflections which are indexed as (001) and (100). The first reflections (d_1) for the two polymers were measured to be 3.79 and 4.00 nm, respectively indicating layer structure. The second reflections (d_2) for them were found to be 1.82 and 1.85 nm, respectively, corresponding to the intermolecular distance including four mesogens. The structure of the mesophase is proposed to be a two-dimensional rectangular structure, where exists some regularity perpendicular to normal layer. This mesophase has been designated as a B_1 phase. As already reported, the compounds with *m*/X/Y = 12/H/H[9] and 7/mono-Cl/H[12] formed a B_1 phase, but the compound with 12/Cl/H[12] only formed a SmC phase. Note that in the case of our polymers *m*/X/Y = 12/Cl/F or 12/Cl/Cl.

Conclusion

The following conclusions can be drawn from the present work.

1. Twelve new azomethine polymers containing banana-shaped mesogenic unit have been synthesized and characterized. The molecular structures were identified by FT/IR and NMR spectroscopy, and the results were in accordance with the expected molecular formula.

2. All of the polymers were soluble only in strong acid such as H_2SO_4 or CF_3CO_2H, etc. The inherent viscosities were in the range of 0.37−0.79 dL/g.

3. All of the polymers were semicrystalline. The values of T_m were in the range 120−224 °C.

4. Four polymers with $m = 6$ (**3b**, **3d**, **3e**, and **3f**) produced a nematic phase on heating, while two polymers with $m = 6$ (**3a** and **3c**) as well as two polymers with m = 12 (**3i** and **3l**) were not thermotropic liquid crystals.

5. Of the polymers with $m = 12$, the mesophase of polymer **3g** has been designated to be a B_2 phase, that of polymer **3h** has been identified as a SmA phase, and those of polymers **3j** and **3k** have been designated as a B_1 phase.

Acknowledgment. This work was supported by Grant No. R01-2001-000-00433-0 from the Basic Research Program of the Korea Science & Engineering Foundation. The X-ray measurements were performed at Pohang Accelerator Laboratory. E-J.C. thanks Professor Edward T. Samulski at the University of North Carolina at Chapel Hill for the discussion about determination of B-phases.

References and Notes

(1) Meyer, R. B.; Liébert, L.; Strzelecki, L.; Keller, P. *J. Phys., Lett.* **1975**, *36*, L-69.
(2) Goodby, J. W. *J. Mater. Chem.* **1991**, *1*, 307.
(3) Tournihac, F.; Blinov, L. M.; Simon, J.; Yablonsky, S. V. *Nature (London)* **1992**, *359*, 621.
(4) Link, D. R.; Natale, G.; Shao, R.; Maclennan, J. E.; Clark, N. A.; Körblova, E.; Walba, D. M. *Science* **1997**, *278*, 1924.
(5) Heppke, G.; Moro, D. *Science* **1998**, *279*, 1872.
(6) Walba, D. M.; Körblova, E.; Shao, R.; Maclennan, J. E.; Link, D. R.; Glaser, M. A.; Clark, N. A. *Science* **2000**, *288*, 2181.
(7) Niori, T.; Sekine, T.; Watanabe, J.; Furukawa, T.; Takezoe, H. *J. Mater. Chem.* **1996**, *6*, 1231.
(8) Workshop on Banana-shaped Liquid Crystals: Chirality by Achiral Molecules, Berlin, Germany, 1997.
(9) Watanabe, J.; Niori, T.; Sekine, T.; Takezoe, H. *Jpn. J. Appl. Phys.* **1998**, *37*, L139.
(10) Shreenivasa Murthy, H.; Sadashiva, B. *Liq. Cryst.* **2002**, *29*, 1223.
(11) Lee, C.-K.; Kim, J.-H.; Choi, E-J.; Zin, W.-C.; Chien, L.-C. *Liq. Cryst.* **2001**, *28*, 1749.
(12) Pelzl, G. Diele, S.; Weissflog, W. *Adv. Mater.* **1999**, *11*, 707.
(13) th FLC Workshop: Banana Liquid Crystals, Chirality & Polarity, Boulder, CO, 2002.

(14) Diele, S.; Grande, S.; Kresse, H.; Lischka, Ch.; Pelzl, G.; Weissflog, W.; Wirth, I. *Ferroelectrics* **1998**, *212*, 169.
(15) Pelzl, G.; Diele, S.; Jákli, A.; Lischka, Ch.; Wirth, I.; Weissflog, W. *Liq. Cryst.* **1999**, *26*, 135.
(16) Coleman, D. A.; Fernsler, J.; Chattham, N.; Nakata, M.; Takanishi, Y.; Körblova, E.; Link, D. R.; Shao, R.-F.; Jang, W. G.; Maclennan, J. E.; Mondainn-Monval, O.; Boyer, C.; Weissflog, W.; Pelzl, G.; Chien, L.-C.; Zasadzinski, J.; Watanabe, J.; Walba, D. M.; Takezoe, H.; Clark, N. A. *Science* **2003**, *301*, 1204.
(17) Lee, C.-K.; Primak, A.; Jákli, A.; Choi, E-J.; Zin, W.-C.; Chien, L.-C. *Liq. Cryst.* **2001**, *28*, 1293.
(18) Sekine, T.; Niori, T.; Sone, M.; Watanabe, J.; Choi, S.-W.; Takanishi, Y.; Takezoe, H. *Jpn. J. Appl. Phys.* **1997**, *36*, 6455.
(19) Sekine, T.; Niori, T.; Watanabe, J.; Furukawa, T.; Choi, S.-W.; Takezoe, H. *J. Mater. Chem.* **1997**, *7*, 1307.
(20) Lee, C.-K.; Chien, L.-C. *Liq. Cryst.* **1999**, *26*, 609.
(21) Thisayuka, J.; Nakayama, Y.; Kawauchi, S.; Takezoe, H.; Watanabe, J. *J. Am. Chem. Soc.* **2000**, *122*, 7441.
(22) Weissflog, W.; Kovalenko, L.; Wirth, I.; Diele, S.; Pelzl, G.; Schmalfuss, H.; Kresse, H. *Liq. Cryst.* **2000**, *27*, 677.
(23) Bodel, J. P.; Ronillon, J. C.; Marcerou, J. P.; Laquerre, M.; Nguyen, H. T.; Achard, M. F. *Liq. Cryst.* **2000**, *27*, 1411.
(24) Kovalenko, L.; Weissflog, W.; Grande, S.; Diele, S.; Pelzl, G.; Wirth, I. *Liq. Cryst.* **2000**, *27*, 683.
(25) Jákli, A.; Nair, G. G.; Lee, C. K.; Sun, R.; Chien, L.-C. *Phy. Rev. E* **2001**, *63*, 061710−1.
(26) Prasad, V. *Liq. Cryst.* **2001**, *28*, 1115.
(27) Keum, C.-D.; Kanazawa, A.; Ikeda, T. *Adv. Mater.* **2001**, *13*, 321.
(28) Matsuzaki, H.; Matunaga, Y. *Liq. Cryst.* **1993**, *14*, 105.
(29) Shen, D.; Diele, S.; Pelzl, G.; Wirth, I.; Tschierske, C. *J. Mater. Chem.* **1999**, *9*, 661.
(30) Dingemans, T.; Murthy, N. S.; Samulski, E. T. *J. Phys. Chem. B* **2001**, *105*, 8845.
(31) th International Liquid Crystal Conference, Edinburgh, UK, 2002.
(32) Lee, C.-K.; Kwon, S.-S.; Chien, L.-C.; Choi, E-J. *Bull. Korean Chem. Soc.* **2000**, *21*, 1155.
(33) Lee, C.-K.; Kwon, S.-S.; Zin, W.-C.; Kim, D.-C.; Shin, S.-T.; Song, J.-H.; Choi, E-J.; Chien, L.-C. *Liq. Cryst.* **2003**, *30*, 415.
(34) Bergel, F.; Reiner, E. *J. Chem. Soc.* **1959**, 2890.
(35) Morgan, P. W.; Kwolek, S. L.; Pletcher, T. C. *Macromolecules* **1987**, *20*, 729.
(36) Wojtkowski, P. W. *Macromolecules* **1987**, *20*, 740.
(37) Pelzl, G.; Diele, S.; Grande, S.; Jákli, A.; Lischka, Ch.; Kresse, H.; Schmalfuss, H.; Wirth, I.; Weissflog, W. *Liq. Cryst.* **1999**, *26*, 401.

MA0348122